Journal of the Korean Nuclear Society
Volume 25, Number 3, September 1993

Air-Water Flooding in Multirod Channels: Effects of Spacer Grids and Blockages

Jong Hee Cha and Hyung Gil Jun
Korea Atomic Energy Research Institute
(Received January 9, 1993)

다봉채널내의 공기-물 플러딩 : 스페이서 그릿 및 블럭키지의 영향

차종희 · 전형길
한국원자력연구소
(1993. 1. 9 접수)

Abstract

This paper presents the experimental results on flooding of countercurrent flow in vertical multirod channels, which consists of falling water film and upward air flow. In particular, the effects of spacer grids, with and without mixing vane, and of blockage in the multirod bundle on the behaviour of flooding were investigated. The 5×5 zircaloy tube bundle was used for the test section. The comparison of previous analytical models and empirical correlations with present data on flooding showed that the existing models and correlations predict much higher flooding curves. The spacer grid causes the lower flooding air flow rate to compare with the bare rod bundle. However, the mixing spacer grids need a higher flooding air flow rate for a constant liquid flow rate than the spacer grids without mixing vanes. The bundle containing blockages has the highest flooding air flow rate among the bundles with spacer grids and blockages. Empirical flooding correlations for the three types of test section have been made.

요 약

이 논문은 하강하는 물의 막과 상승하는 공기유동으로 구성된 수직 다봉채널내서의 역유동 플러딩에 관한 실험결과를 발표한 것이다. 특히 다봉속에 혼합깃이 있는 것과 없는 스페이서 그릿 및 블럭키지가 프러딩의 거동에 미치는 영향이 조사되었다. 시험부에는 5×5 지르칼로이관속이 사용되었다. 플러딩에 관한 전의 해석적 모델과 실험적 상관식들을 본 실험결과와 비교한즉 기존의 모델과 상관식들이 매우 높은 플러딩 곡선을 예측함이 발혀졌다. 스페이서 그릿은 이것이 없는 봉속과 비교하면 낮은 플러딩 공기유량을 나타낸다. 그러나 혼합깃이 있는 스페이서 그릿은 이것이 없는 스페이서 그릿에 비하여 높은 플러딩 공기유량이 요구된다. 블럭키지를 가진 봉속은 더욱더 높은 플러딩 공기유량을 갖는다. 세가지 형식의 시험봉 속에 대한 실험적 플러딩 상관식이 얻어졌다.

1. Introduction

There are some systems in a nuclear reactor in which the flooding phenomena may occur during the reflood process following a hypothetical loss-of-coolant accident. One of the important cases is the reactor core itself, which can be cooled by liquid injected into the upper plenum and subsequently falling into the core. In this case, the flooding phenomena may cause a limitation of the downward penetration of the emergency core cooling liquid flow due to the partial blockage by the updrafting vapor generated in the heated core. In an extreme case, a high vapor flow may cause reversal of the liquid flow. Therefore, the flooding phenomenon is an important concern in safety assessment of nuclear reactors.

The objective of the present work is to investigate experimentally countercurrent flooding in a vertical multirod channel which consists of falling water film and upward air flow. In particular, the effects of various spacer grids, with and without mixing vanes, and of blockages in the multirod bundle on the behaviour of flooding are investigated. There is a large volume of literature concerning the theoretical analyses and experimental studies on vertical two-phase countercurrent flooding. However, most previous studies on flooding concentrated on a single channel test section. In spite of the importance of practical application, there are only limited informations reported in the open literature on flooding in multirod channel. Moreover, no experimental data are currently available regarding the influence of spacer grids with and witnout mixing vanes on flooding in multirod channels.

In connection with the multi-channel flooding tests, Hagi[1] performed tests in parallel channels, and Speyer and Kmetyk [2] did flooding tests for a four channel test section. The results of both tests showed that the Wallis correlation [3] for single channel did not give good agreement. They pointed out that all single channel correlations must be modified to incorporate the multi-channel effect. Ueda and Suzuki[4] performed air-water flooding experiments in annular and rod bundle geometries. They have made a correlation based on the Froude number. Liu, McCarthy, and Tien[5] performed experiments on the onset of flooding with air-water for various multipath contraction plates. They primarily investigated the effects of the contraction plate geometry conditions on the flooding. Recently, Kokkonen and Tuomisto[6] performed air-water flooding experiments across perforated upper tie plates in multirod channel geometries. They correlated the various flooding equations using Kutateladze numbers with their flooding data. However, their experiments were mainly concentrated on the effects of the presence of the perforated upper tie plates in the multirod bundle.

There are some experimental results on flooding in the upper core structures and downcomers of nuclear reactors. Tobin[7] performed experiments with steam and water in the upper tie plate open area of a BWR fuel bundle. Sun and Fernandez[8] correlated Tobin's data with a Kutateladze-type correlation. Jones[9] performed another series of tests with steam and water in the upper region of a BWR fuel bundle. Test results showed that the method of liquid injection moderately influences the flooding results. Crowley et al.[10] carried out the flooding tests using a 1/5 scale PWR downcomer model, and they developed an empirical correlation. Schmacher et al. [11] found the temperature peak at the upper part of the flooding region in a series of experiments with steam and water in the test model of a BWR upper tie plate. Glaeser[12] developed different correlations for the flooding in the downcomer and tie plate based on the experimental data obtained from the tests in the Upper Plenum Test Facility in Germany. Recently, Chun et al. [13] investigated the flooding of air-water coun-

tercurrent flow in a vertical 3×3 tube bundle with an egg-crate type spacer grid. They found that the Kutateladze flooding correlation overpredicts the flooding gas velocities in the multirod bundle with spacer grid.

2. Experimental Apparatus and Procedure

The experimental apparatus consisted of two systems : the fluid flow system and instrumentation system. The fluid flow system was designed to circulate air and water in the apparatus and to form a vertical air-water countercurrent flow in the test section. The instrumentation system was utilized to measure and store the air and water flow rates and pressure drops through the test section. A schematic diagram of the experimental apparatus is shown in Figure 1.

The fluid flow system consisted of a test section, an upper and a lower plenum, and the air and water circulation and control system. The outer wall of the test section was made up of a transparent plexiglas channel 6.3×6.3 cm square and 150 cm in height. The 5×5 zircaloy tube bundle was placed vertically in the plexiglas square channel. The tube array had the same geometrical dimensions as a typical 17×17 PWR fuel bundle. The outside diameter of each tube and the tube pitch were 9.5 and 12.6 mm, respectively. The upper and lower plena were installed at the top and bottom of the test section. Both of the plena were made of stainless steel. The upper plenum provided a support for the upper part of test section and a means of separating water carry-over from the air flow. The lower plenum supported the test section and housed the air and water inlets. The two inlets were designed in such a way that a direct interaction between two fluids can be avoided. Figure 2 shows the details of the test section.

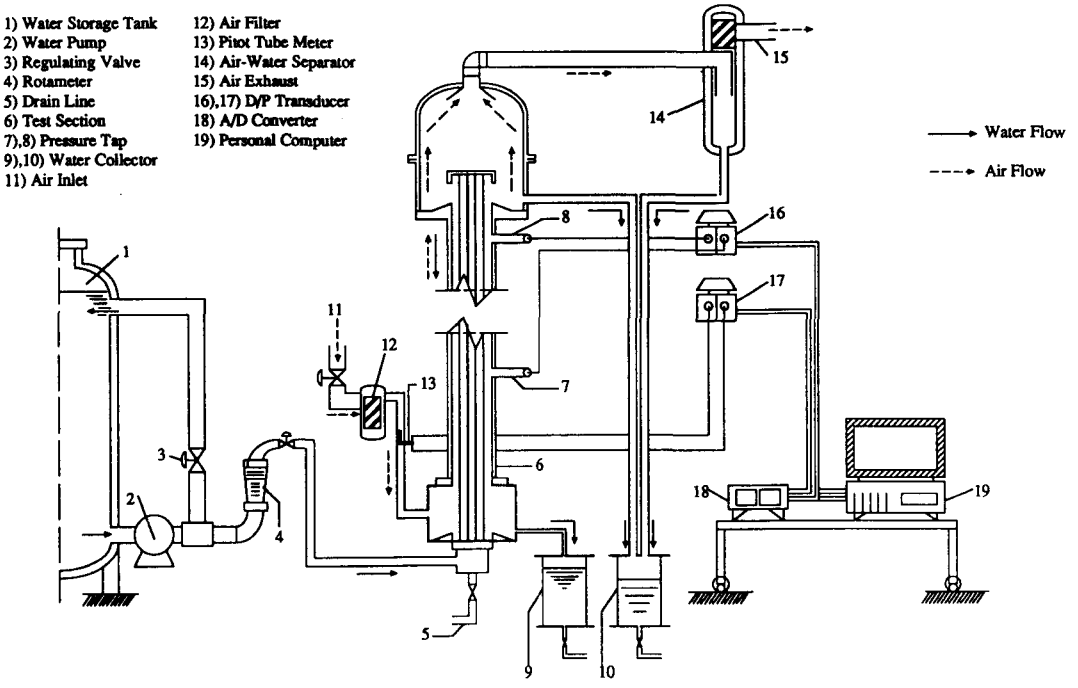

Fig. 1. Schematic Diagram of Test Loop

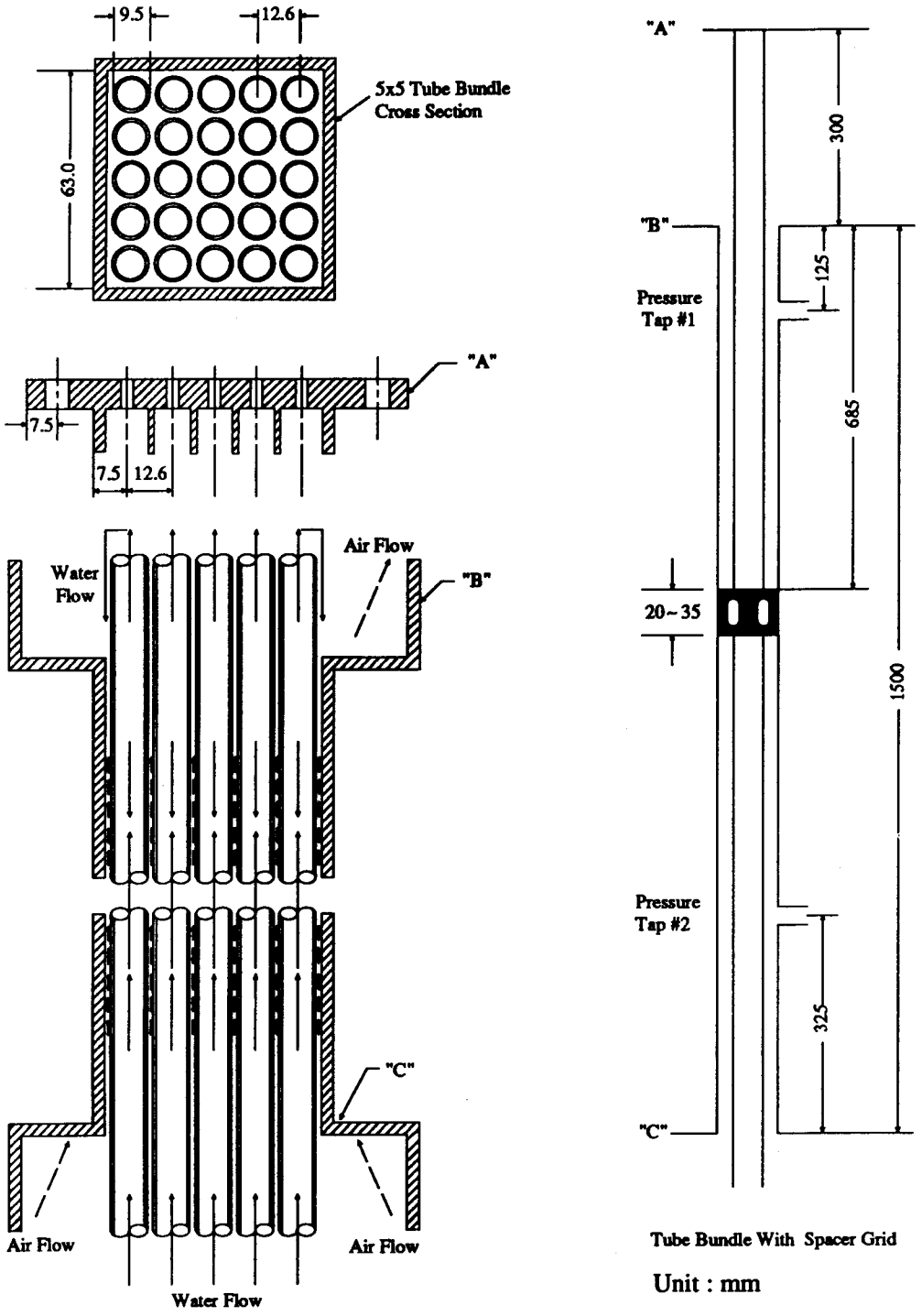

Fig. 2. Details of Test Section

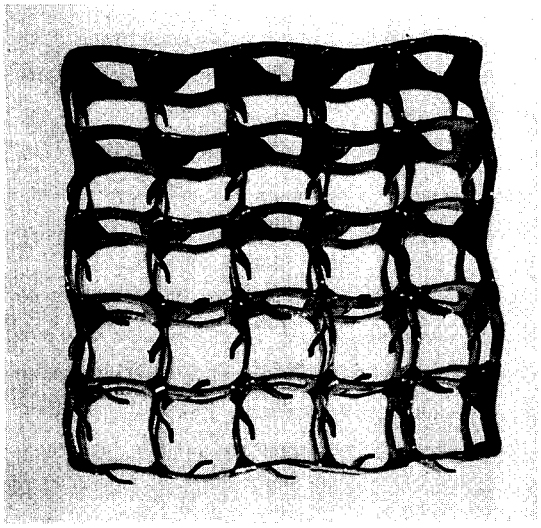

Standard Spacer Grid

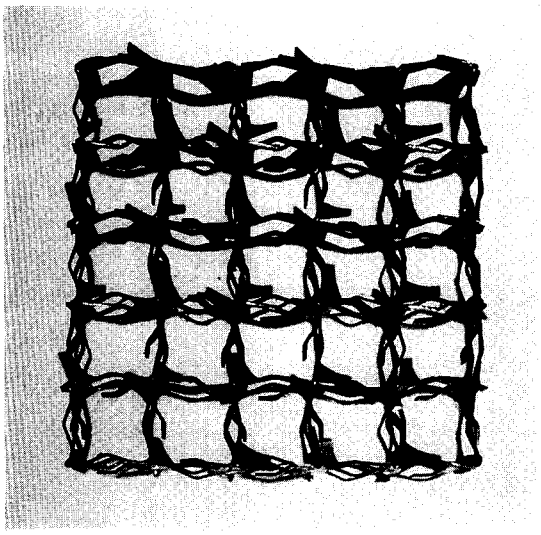

Wavy Split Vane Spacer Grid

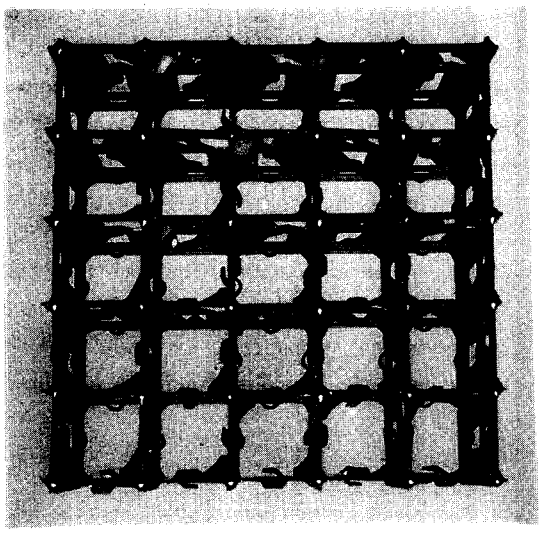

Inverted Vane Spacer Grid

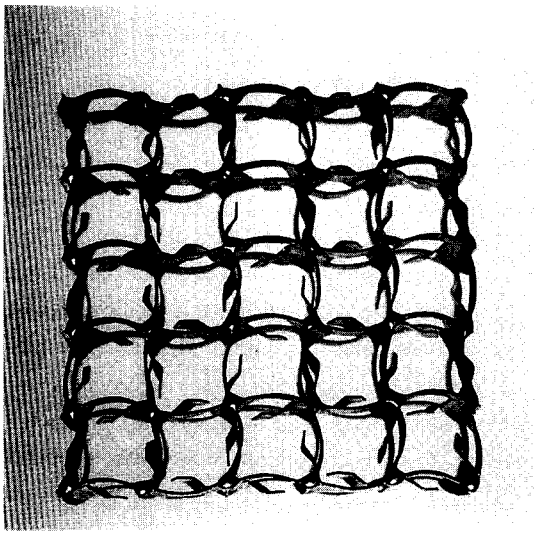

Inclined Wave Spacer Grid

Fig. 3. Photographs of Various Spacer Grids

To obtain the experimental informations on the effects of spacer grid and blockage in multirod channel on the flooding behavior, four types of spacer grids as shown in Figure 3, and nine blocked rods arrangement as in shown in Figure 4, were used. Among them, the standard spacer grid(SSG) does not contain mixing vanes, whereas the other three, inclined wave spacer grid(IWSG), wavy split vane spacer grid(WSVSG), and inverted vane spacer grid(IVSG), do contain mixing vanes.

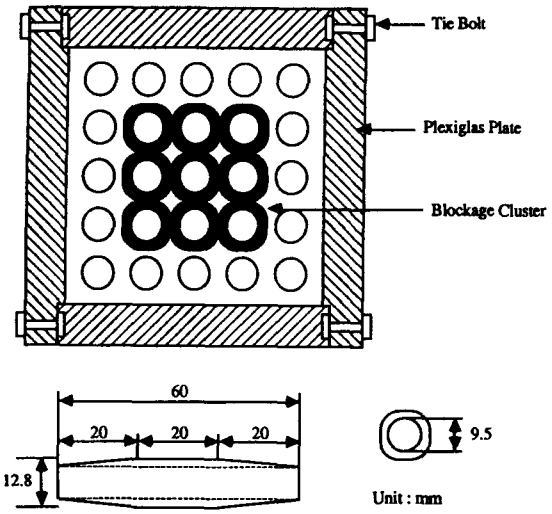

Fig. 4. Details of Blockage and Cross Sectional View of Test Channel with Blockages

The samples of spacer grids were donated by ABB Combustion Engineering.

Air was supplied to the apparatus from the laboratory supply at about 0.5 MPa. A pressure regulator provided a constant upstream pressure of 0.1 MPa. The air flowed through the test section into the upper plenum and was exhausted to the atmosphere after passing through the upper plenum and air–water separator. The air flow rate was determined by Pitot tube meter pressure drops, which were indicated by the differential pressure transducers output. Water was supplied to the test section through a rotameter by a centrifugal–type water pump. The water flow rate was measured by a rotamter. The water was first introduced into the inlet located at the bottom of the lower plenum, then it rose up to the top of the bundle flowing inside of each tube. The water flowing out of the 25 tubes at the top was then directed, by the nozzle, to flow in the reverse direction downward by gravity over the outer surface of 25 tubes forming a continuous annular water film. The nozzle was placed 30 cm above the top of test channel in order to form a fully developed flow. The pressure drop in the test section was measured by a pressure transducer, and its output was stored on the personal computer. Any water which was separated from the upper plenum and the air–water separator was drained into a collector for the carry–over water. The water which penetrated through the test section was drained into another collector.

In each of the flooding tests, a steady water flow rate was established. Then a low air flow rate was introduced. Both the air and water flow rates were maintained at constant levels for about 5 minutes to ensure that steady–state had been reached. Next, the air flow rate was increased in small steps, and so forth. The range of these steps included operation from complete water penetration to nearly complete water entrainment. During this step operation, the onset of flooding could be readily found by visual observation and pressure drop tracing data. The onset of flooding corresponds to the onset of water carry–over. At the end of a test with a fixed water flow rate, the air flow was shut off, and a new water flow rate was established for the next test.

Major quantities measured for each test were water inlet flow rate, air inlet flow rate, water penetration rate, water carry–over rate and test channel pressure drop. Test conditions are shown in Table 1.

Table 1. Test Conditions

Maximum Flow Rate (Kg/sec)	Temperature (K)	Test Pressure (MPa)	Examined Spacer Grid
Air : 0.04	Air : 288	0.1	SSG
Water : 0.17	Water : 283		WSVSG
			IVSG
			IWSG

3. Experimental Results and Discussion

3.1. Observation of Flooding Process

Visual observations of the phenomena in the test section are useful to understand the flooding process. For the bared (no spacer grid) multirod bundle test section, four distinct flow regimes were observed with increase of the air flow rate at a constant water flow rate : separated two-phase countercurrent flow, water slug formation in the bottom of the test section with wavy annular water flow, water slug formation in the bottom of the test section with partial climbing flow of water film, and complete water carry-over. The water slug formation phenomenon is sometimes called "air-water mixed flow"[14]. The third flow regime is herein called the onset of flooding. The flooding is associated with a sudden increase of water carry-over with a small increase in air flow rate. The onset of flooding is always initiated at the lower part of the test section in the case of the bared bundle. The fourth flow regime is completely upward cocurrent two-phase flow configuration.

The flooding process in the multirod bundle with spacer grid is almost similar to that in the bared bundle except for the shift of the flooding initiation level. For the multirod bundle with the spacer grid test section, the flooding first occurred at the upper side of the spacer grid. Figure 5 shows a set of photographic view of the flow regimes in the multirod bundle with spacer grid test section. Figure 5(a) is a view of separated two-phase countercurrent flow. Figure 5(b) shows water slug formation at the upper side of the spacer grid with wavy annular water flow in the upper part of the test section. Figure 5(c) shows a view of the onset of flooding in the upper part of the spacer grid. Finally, Figure 5(d) shows a complete water carry-over flow configuration. It was observed that there was no significant difference in flow configuration between the spacer grids with and without mixing vanes. A similar trend was also observed in the bundle containing blockages.

An important characteristics of the flooding phenomena is the appearance of a large disturbance at the gas-liquid interface. The pressure drop tracing provides detailed information about the interaction between gas and liquid, and it may be used to complement the visual observations. Many investigators observed a sudden increase in the pressure drop after the onset of flooding due to the abrupt increase of the interfacial drag force between the gas flow and the entrained liquid droplets. The traces of pressure drop during the flooding process for the bared bundle and the spacer grid(SSG) attached bundle under the same condition of 0.056 kg/sec water flow rate are shown in Figure 6. As seen in this figure, these pressure drop curves are significanly different in those shapes. For the bared bundle, the pressure drop rises sharply up to maximum value at the air velocity corresponding to the onset of flooding. Further increases in the air velocity tend to decrease the pressure drop because the climbing water film appears to form a cocurrent two-phase flow. A similar result was previously obtained by Hawley and Wallis[15] in a vertical single tube. For the spacer grid attached bundles, the jump of pressure drop occurred at a substantially lower flooding air velocity, and the height of the jump is remarkably less than that in the bared bundle. After the jump, pressure drop is still gradually increased up to maxinum value with increasing he air velocity. The total amount of pressure drop in the bundle with spacer grids is somewhat smaller than that in the bared bundle. This difference may be attributed to a shift in the location of flooding occurence in the bundle with the spacer grids. The shift of the flooding point shortens the length of the flooding region, resulting in a lower pressure drop.

In Figure 7, the interfacial friction factors deduced from the pressure drop data for various multirod bundles during the flooding process under the condition of 0.056 kg/sec water flow rate are shown as a function of liquid void frac-

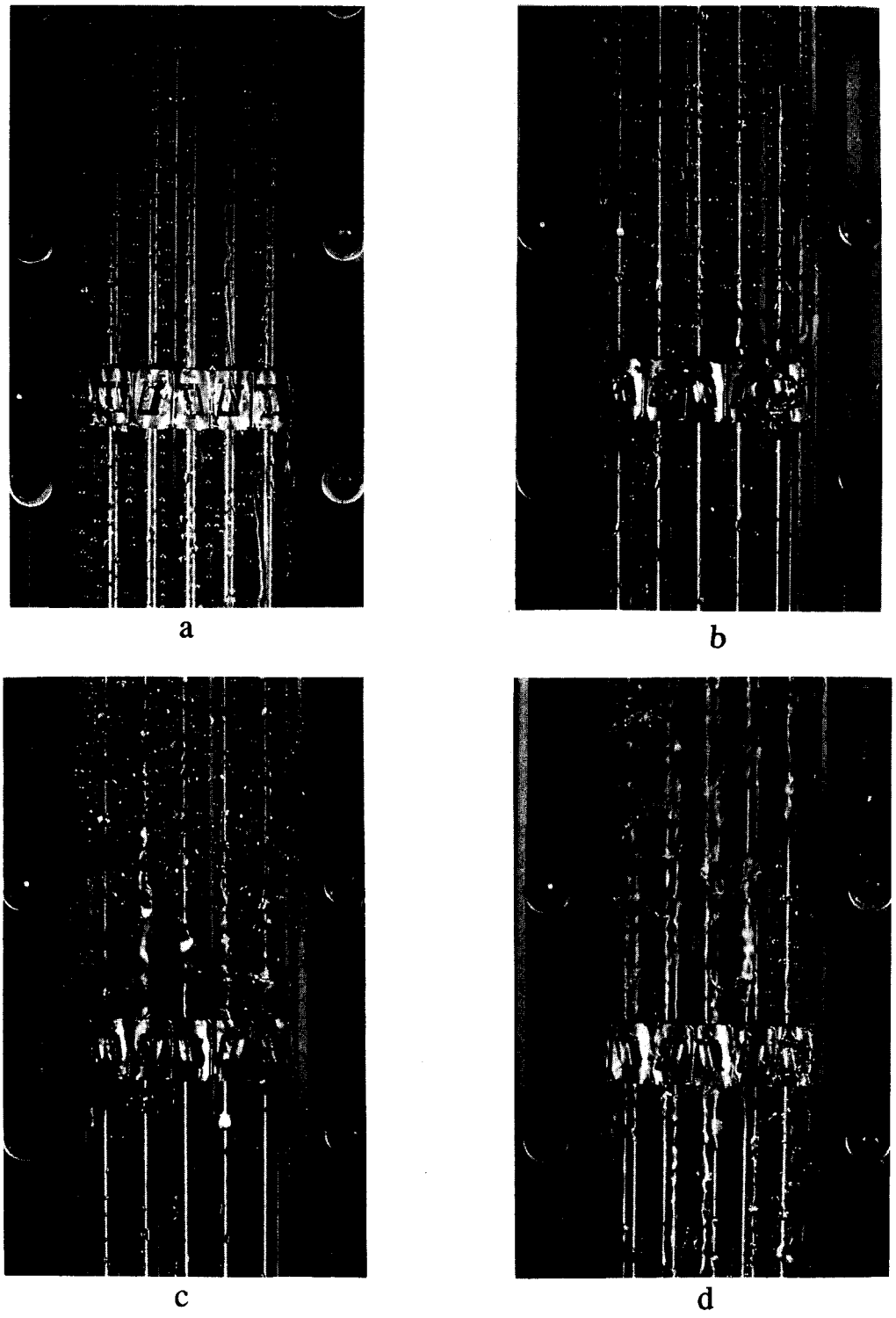

Fig. 5. Photographical View of Flooding Process in Multirod Channels with Spacer Grid

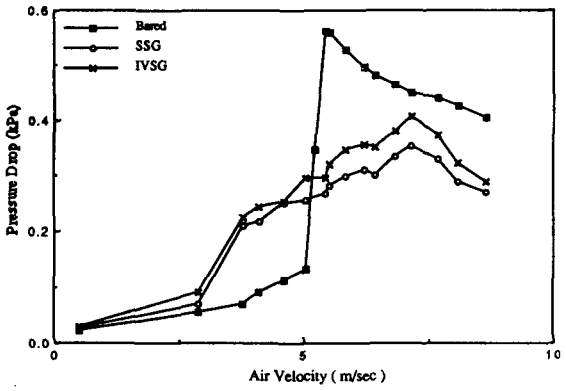

Fig. 6. Pressure Drop Variation with Air Flow Rate During Flooding Process

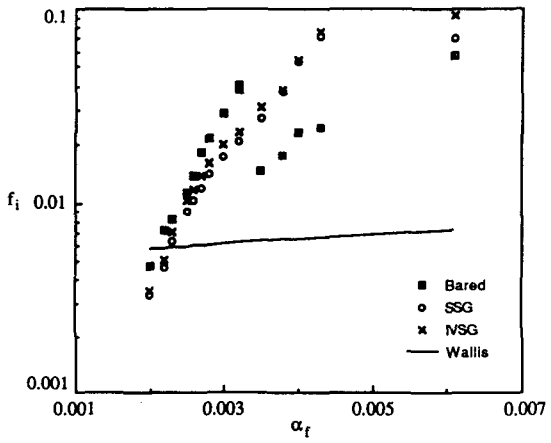

Fig. 7. Interfacial Friction Factor with Liquid Fraction for Various Rod Conditions(Water Flow Rate : 0.056kg/sec)

tion. The interfacial friction factor was calculated by considering the force balance for an assumed gas core[16]. As seen in this figure, most of the calculated friction factors lie much higher than the Wallis correlation curve[3].

3.2. Comparison with Previous Models and Correlations

Comparisons of present flooding data with some previous analytical models and empirical correlations are shown in Figure 8. For these comparisons, the Wallis parameters were chosen as the basic variables because most analytical models and empirical correlations are expressed in terms of these parameters. Present experimental data are included herein for the bared bundle and for the bundle with standard spacer grid. The selected analytical models are : a) potential flow model[17], b) roll wave model[18], and c) separated cylinders model[19]. Two correlations developed by Wallis[3] and Chung et al.[20] are selected. These are mostly for single tube. For the present test section geometry, the equivalent diameter in the Wallis parameter was calculated in the following way :

$$De=\frac{4A}{4B+n\pi d} \quad (1)$$

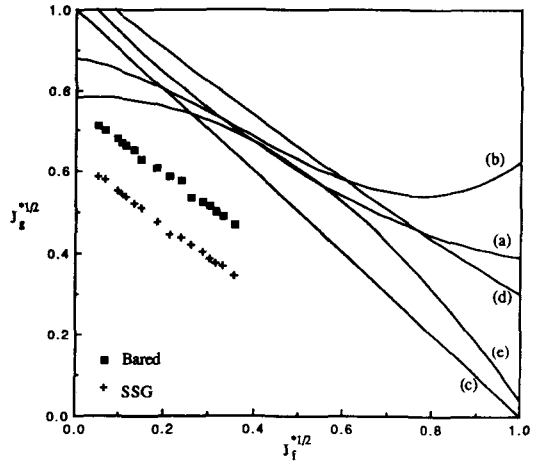

Fig. 8. Comparison of Present Flooding Data with Various Analytical Models and Empirical Correlations
(a) Potential Flow Moder
(b) Roll Wave Model
(c) Separate Cylinders Model
(d) Chung et al.
(e) Suzuki and Ueda

where A is the flow cross sectional area, B is the inside width of the test section, n is the number of rods, and d is the tube outer diameter.

As shown in Figure 8, most of the present flooding points lie under the existing analytical and empirical flooding curves. This means that the flooding for the multirod channels occurred at lower gas flow rate with a fixed liquid flow rate compared to the single channel. This may be attributed to disturbance of the liquid flow due to the interaction of liquid films between adjacent channels.

A comparison of the present flooding data in the bundle with spacer grid to the bared bundle shows that the former lies under the latter in Figure 8. It appears that the spacer grid acts to rupture the stable liquiuid film partially, and to lead to the formation of liquid slugs and/or bridging at the upper side of the spacer grid. The chaotic state can easily reach the flooding condition even at lower gas flow rates.

The Wallis correlation[3] represents gas momentum flux versus liquid momentum flux versus liquid momentum flux under the flooding conditions as follows,

$$J_g^{*1/2}+mJ_f^{*1/2}=C \tag{2}$$

$$J_k^*=j_k\left[\frac{\rho_k}{\rho De(\rho_f-\rho_g)}\right]^{1/2} \tag{3}$$

where constants m and C in the equation are determined by experiment. In the present experiments,

for the bared bundle, m=0.80 and C=0.76

for the SSG bundle, m=0.80 and C=0.63

where obtained. During the data process, the effect of spacer grid was taken into account for the calculation of superficial velocity.

3.3. Effects of Mixing Spacer Grids and Blockages

In a tube bundle, flow channels formed by four adjacent tubes are open to each other through the gap between two neighboring tubes. The flow in one channel mixes with that of the others. One of the functions of the spacer grid containing mixing vane, simply called the mixing spacer grid here, is to enhance the mixing effect in the flow channel. In order to investigate the degree of mixing effect in the flow channel with the mixing spacer grids or the blockages, separate flow tests[21] were conducted with the present test model with water using the Laser Doppler Velocimeter. Figure 9 shows the typical measured turbulent intensity as a function of transverse location of the test section. The turbulent intensity which is represented the degree of mixing, T is defined as:

$$T=\frac{v}{\overline{U}}\times 100 \tag{4}$$

where v is the measured transverse instantaneous velocity, and U is the average axial velocity in the test channel flow.

The value of the turbulent intensity depends on the flow conditions as well as on the axial location in the channel, but the general trend is similar. As seen in Figure 9, the lowest value can be found at the SSG bundle, and then it increases in the order of WSVSG, IWSG, and IVSG. The IVSG bundle has a relatively high degree of mixing effect. It should be noted that the highest turbulent intensity appears at the mid region of the blocked bundle.

In the flooding process, air flow is dispersed by the mixing spacer grid. It appears that the amount

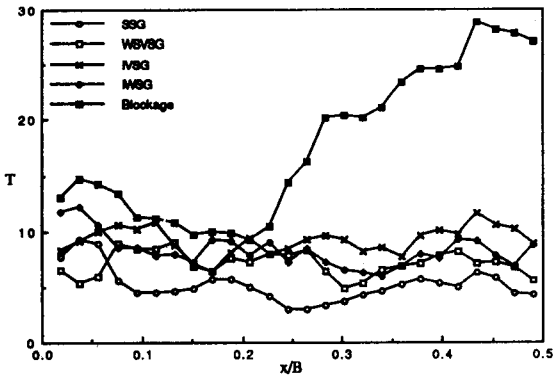

Fig. 9. Turbulent Intensity Variations for Each Type of Bundle

of this dispersion directly relates the magnitude of turbulent intensity, and the turbulence prevents the formation of water slug at the upper part of the mixing spacer grid. Consequently, the required flooding air flow rate must be increased for the mixing spacer grid. The present flooding data on the effects of mixing spacer grids and blockages will be presented in the later section.

3.4. Empirical Correlations of Flooding Data

The other type of flooding correlation takes into account the interfacial instabilities. The geometric length in the Wallis parameter can be replaced a Laplace Length to obtain the following Kutateladze number[22] :

$$K_k=\bar{U}_k\left[\frac{\rho_k^2}{g\sigma(\rho_f-\rho_g)}\right]^{1/4} \quad (5)$$

Several investigators prefer to use the following correlation form for the flooding data, especially for nuclear reactor structures, based on the Kutateladze number,

$$K_g^{1/2}+mK_f^{1/2}=C \quad (6)$$

Figure 10 shows the whole set of experimental data from the present tests on air-water flooding in the K_g versus K_f plane. Three experimental flooding curves are plotted for bared, SSG, and IVSG bundles and are compared with CREARE [10] and Chung et al.[20] correlations. From these experimental curves, the following Kutateladze type empirical flooding correlations for bared, SSG, and IVSG bundles are obtained :

$$\text{for bared bundle : } K_g^{1/2}+0.8K_f^{1/2}=1.39 \quad (7)$$

$$\text{for SSG bundle : } K_g^{1/2}+0.8K_f^{1/2}=1.16 \quad (8)$$

$$\text{for IVSG bundle : } K_g^{1/2}+0.8K_f^{1/2}=1.24 \quad (9)$$

As shown in Figure 10, the slopes of experimental flooding curves for present data are

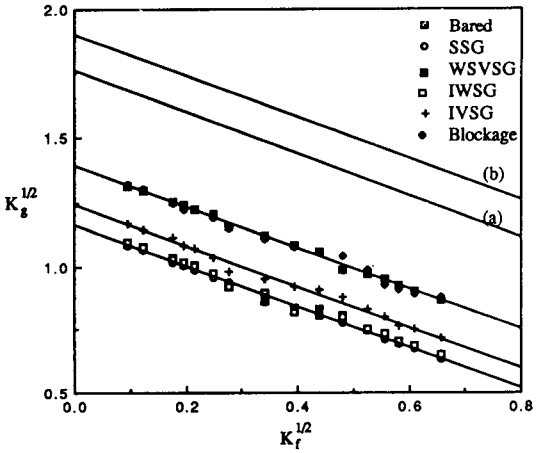

Fig. 10. Comparison of Present Flooding Data with Previous Correlations (a) Chung et al.(b) CREARE

similar to those of previous correlations. However, the existing Kutateladze flooding correlations greatly overpredict the flooding gas mass flux compared with the data multirod channel. As suggested by Speyer and Kmetyk[2], the existing flooding correlations for single channel must be modified to incorporate the multi-channel effect.

In connection with the flooding data in the multirod bundle with mixing spacer grid or blockage, the flooding air mass flux increased in the order of turbulent intensity increasing at a constant water mass flux. As mentioned in the above section, this trend may be attributed primarily to the effect of air dispersion by the mixing spacer grids or blockages.

4. Conclusions

An experimental study of air-water flooding in vertical multirod channel has been performed. This study was especially focused primarily on the effects of various spacer grids and blockages in the multirod bundle. Based on the results of this study, the following conclusions could be made : (1) For the multirod bundle with the spacer grid,

flooding first occurred at the upper side of the spacer grid, whereas flooding is initiated at the bottom of the test section for the bared bubndle.

(2) The existing analytical models and correlations on flooding, mainly for single channel, over-predict the flooding gas mass flux compared with the data for the multirod channel.

(3) For the spacer grid, the flooding phenomenon occurs at the lower flooding air mass flux to compare with the bare rods.

(4) In the multirod bundle with mixing spacer grid or blockage, the flooding air mass flux increased in the order of turbulent intensity increasing at a constant water mass flux. Generally, the mixing spacer grid needs the higher flooding gas mass flux at a fixed liquid mass flux than the spacer grid without mixing vane.

(5) The highest mixing effect appears at the bundle containing blockage during the present experiments.

(6) Kutateladze type flooding correlations can be made based on the present data.

Nomenclature

A	cross sectional flow area of test section, m^2
B	inside width of test section, m
C	empirical constant
d	outer diameter of tube, m
D_e	equivalent diameter of flow channel, m
f	friction factor
g	gravitational acceleration, m/sec^2
j	superficial velocity, m/sec
J^*	dimensionless parameter defined by Eq.(3)
K	dimensionless number defined by Eq.(5)
m	empirical constant
T	turbulent intensity defined by Eq.(4)
U	axial velocity, m/sec
v	transverse velocity, m/sec
x	coordinate
α	void fraction
ρ	density, kg/m^3

Subscripts

f	liquid
g	gas
i	interfacial
k	g or f

References

1. Y. Hagi, "Air-water Flooding for Parallel Channel Flows Based on the Results for Single Path Flows," *M.S. Thesis,* Dartmouth College, (1976)
2. D.M. Speyer and L. Kmetyk, "Flooding in Multi-channel Two-Phase Counter-Flow," *Nuclear Reactor Safety Heat Transfer,* pp.55-62, ASME, New York, (1977)
3. G.B. Wallis, *One Dimensional Two-Phase Flow,* Mc Graw-Hill, (1969)
4. T. Ueda and L. Suzuki, "Behavior of Liquid Films and Flooding in Countercurrent Two-Phase Flow, Part 2, Flow in Annuli and Rod Bundles," *Int. J. Multiphase Flow,* **4**, p.157, (1978)
5. C.P. Liu, G.E. McCarthy, and C.L. Tien, "Mixing and Flooding in Vertical Gas-Liquid Countercurrent Flow Through Parallel Paths," *EPRI Report NP-2262,* (1982)
6. I. Kokkonen and H. Tuomisto, "Countercurrent Flow Limitation Experiments with Full-Scale Fuel Bundle Structure," *Proc. Fourth Internationsl Topical Meeting on Nuclear Reactor Thermal Hydraulics,* Karlsruhe, pp.82-87, October, (1989)
7. R.J. Tobin, "CCFL Test Results-Phase 1-TLTA 7×7 Bundl, C.E. BWR/ECC Program," *7th Monthly Report,* (1977)

8. K.H. Sun and R.T. Fernandez, "Countercurrent Flow Limitation Correlation for BWR Bundles during LOCA", *Trans. ANS,* **27**, p.625, (1977)
9. D.D. Jones, "Subcooled Countercurrent Flow Limiting Characteristics of the Upper Region of a BWR Fuel Bundle," *NEDG–23549*, (1977)
10. C.J. Crowley, P.H. Rothe, and R.G. Sam, "1/5 Scale Countercurrent Flow Data Presentation and Discussion : CREARE, Inc.," *NUREG/CR–2106*, (1981)
11. D.G. Schmacher, T. Eckert and J.A. Findlay, "BWR Refill–Reflood Program Test Results : CCFL–Refill System–Effects(30°Sector)," *EPRI Report, NP–2374,* January, (1984)
12. H. Glaeser, "Analysis of Downcomer and Tie Plate Countercurrent Flow in the Upper Plenum Test Facility," *Proc. Fourth International Topical Meeting on Nuclear Reactor Thermal Hydraulics,* Karlsruhe, pp.75–81, October, (1989)
13. Moon–Hyun Chun, Bub Dong Chung and Jong Hee Cha, "Experimental Investigation of Flooding in Air–Water Counter–Current Flow with a Vertical Adiabatic Multi–rod Bundle," Advances in Gas Liquid Flows, ASME FED–Vol.99, pp.237–242, 1990
14. H.M. Lee, G.E. MaCarthy, and C.L. Tien, "Liquid Carry–over and Entrainment in Air–Water Counter–current Flooding," *EPRI Report, NP–2344,* April, (1982)
15. D.L. Hawley and G.B. Wallis, "Experimental Study of Liquid Film Fraction and Pressure Drop Characteristics in Vertical Countercurrent Annular Flow," *EPRI Report, NP–2280,* (1982)
16. D. Barathan, G.B. Wallis, and H.J. Richer, "Air–Water Countercurrent Annular Flow," *EPRI Report, NP–1165,* September, (1979)
17. H. Imura, H. Kusada, and S. Funatsu, "Flooding Velocity in a Countercurrent Annular Two–Phase Flow," *Chem. Eng. Sci.,* **32**, pp.79–87, (1977)
18. H.J. Richer, "Flooding in Tubes and Annuli," *Int. J. Multiphase Flow,* **7**, pp.647–658, (1981)
19. G.B. Wallis, "Flooding Velocities for Air and Water in Vertical Tubes," *AAEW–R123,* UKAEA, England, (1961)
20. K.S. Chung, L.P. Liu, and C.L. Tien, "Flooding in Two–Phase Countercurrent Flows, Ⅱ. Experimental Investigation," *Physicochem, Hydrodyn.,* **1**, pp.209–220, (1980)
21. M.K. Chung, et al., "Hydraulic Tests on Mixing Vane Contained Spacer Grids in 5×5 Multirod Bundle Using LDV Technique," *KAERI/TR–173–90*, (1990)
22. O.L. Puschkina and Y.L. Sorokin, "Breakdown of Liquid Film Motion in Vertical Tubes," *Heat Transfer–Soviet Research 1,* **5**, pp.56–64, (1969)